JOURNAL OF APPLIED PHYSICS VOLUME 91, NUMBER 6 15 MARCH 2002

C lattice site distributions in metastable $Ge_{1-y}C_y$ alloys grown on Ge(001) by molecular-beam epitaxy

S. Y. Park, J. D'Arcy-Gall, D. Gall,[a] Y.-W. Kim, P. Desjardins,[b] and J. E. Greene
Department of Materials Science and the Frederick Seitz Materials Research Laboratory, University of Illinois, 104 South Goodwin Avenue, Urbana, Illinois 61801

(Received 28 September 2001; accepted for publication 4 December 2001)

Epitaxial metastable $Ge_{1-y}C_y$ alloy layers with $y \leqslant 0.045$ were grown on Ge(001) by solid-source molecular-beam epitaxy (MBE) at temperatures $T_s = 200–400\,°C$. Using calculated strain coefficients and measured layer strains obtained from high-resolution reciprocal lattice maps (HR-RLMs), we determine C lattice site distributions as a function of T_s and total C concentration y. HR-RLMs show that all as-deposited alloys are fully coherent with their substrates. $Ge_{1-y}C_y(001)$ layers grown at $T_s \leqslant 350\,°C$ are in a state of in-plane tension and contain C in substitutional sites, giving rise to tensile strain, as well as in nanocluster sites which induce negligible lattice strain. $T_s = 400\,°C$ layers are strain neutral with negligible substitutional C incorporation. Increasing y and/or T_s leads to a decrease in substitutional C concentration, consistent with Raman spectroscopy results, with a corresponding increase in the C fraction incorporated in nanocluster sites. The latter suggests that nanocluster formation is kinetically limited during film deposition by the C–C adatom encounter probability at the growth surface. Overall, the results show that it is not possible by MBE to obtain fully substitutional C incorporation in $Ge_{1-y}C_y(001)$ alloys, irrespective of y and T_s. This is consistent with *ab initio* density functional calculations results showing that C incorporation in nanoclusters sites is energetically favored over incorporation in substitutional Ge lattice sites. Annealing the $Ge_{1-y}C_y(001)$ layers at $T_a = 550\,°C$ leads to a significant decrease in the substitutional C fraction and, hence, lower tensile strain. Layers annealed at 650 °C are strain free as all substitutional C has migrated to lower-energy nanocluster sites. © *2002 American Institute of Physics.* [DOI: 10.1063/1.1448677]

I. INTRODUCTION

C-containing group-IV alloys are of technological and scientific interest due to the potential they offer for both band gap and strain-state engineering of layers used in microelectronic and optoelectronic devices compatible with Si integrated circuit technology. There are, however, severe challenges associated with their growth. First, the equilibrium solid solubilities of C in Si and Ge are extremely low, $\simeq 10^{17}\ \mathrm{cm}^{-3}$ and $10^{8}\ \mathrm{cm}^{-3}$, respectively.[1] Low-temperature growth under highly kinetically constrained conditions is therefore required in order to take advantage of the fact that surface solubilities are orders of magnitude larger than bulk values,[2] while simultaneously inhibiting phase separation during deposition. Another obstacle to be overcome is the large lattice constant mismatch, 34% and 37%, between diamond ($a_C = 3.5668$ Å) and the common group-IV semiconductors Si ($a_{Si} = 5.4310$ Å) and Ge ($a_{Ge} = 5.6576$ Å).

$Si_{1-y}C_y$ has been widely studied experimentally and theoretically, but C incorporation in $Ge_{1-y}C_y$ alloys has received relatively little attention. Most reported experimental investigations have focused on the growth of $Ge_{1-y}C_y$ layers ($y \leqslant 0.1$) on Si(001).[3,4] However, $Ge_{1-y}C_y$/Si(001) layers typically have highly defective microstructures containing large concentrations of misfit dislocations which can act as sinks for incorporated C. These samples are thus unsuitable for investigating C incorporation pathways in $Ge_{1-y}C_y$.

There are few reports of the successful growth of metastable $Ge_{1-y}C_y$ alloys on Ge(001). Duschl *et al.*[5] employed solid-source molecular-beam epitaxy (MBE) to grow thirty periods of 30 Å-$Ge_{1-y}C_y$/100 Å-Ge superlattices with $y = 0.012$ and 0.021 at temperatures $T_s = 200$ and 300 °C. The authors stated that 30% of the total C concentration resided in substitutional sites at $T_s = 200\,°C$ with only 10% at 300 °C. The substitutional fractions were estimated based upon strain values obtained from x-ray diffraction measurements. Dashiell *et al.*[6] demonstrated in-plane tension in $Ge_{1-y}C_y$/Ge(001) layers grown by MBE at $T_s = 275\,°C$, but did not measure y.

Yang *et al.*[3] reported the growth of epitaxial $Ge_{0.95}C_{0.05}$ on Ge(001) by MBE at $T_s = 200\,°C$ and noted that the layers were highly defective with rough {113} facetted surfaces. Raman spectroscopy indicated that only a small fraction of the C was in substitutional sites giving rise to a local vibrational mode at $530\ \mathrm{cm}^{-1}$ (Ref. 7). The peak position is in good agreement with an investigation by Hoffman and co-workers[8] who used ion channeling and infrared absorption spectroscopy to characterize Ge wafers implanted with $^{12}C^{+}$ and $^{13}C^{+}$ ions at energies and doses chosen to provide a relatively uniformly doped 0.7 μm-thick region with $y = 0.007$. They observed a Ge–C stretch mode at a frequency

[a]Electronic mail: d-gall@uiuc.edu
[b]Permanent address: Groupe de recherche en physique et technologie des couches minces, Département de génie physique, École Polytechnique de Montréal, P.O. Box 6079, Station Centre-Ville, Montréal, Québec H3C 3A7, Canada.

0021-8979/2002/91(6)/3644/9/$19.00 © 2002 American Institute of Physics

Downloaded 28 Feb 2002 to 130.126.102.15. Redistribution subject to AIP license or copyright, see http://ojps.aip.org/japo/japcr.jsp

of 531 cm^{-1}, consistent with values between 516 and 563 cm^{-1} obtained from local density functional calculations of the vibrational mode frequencies of substitutional C in Ge. Analyses of channeling rocking curves around the ⟨100⟩, ⟨110⟩, and ⟨111⟩ axes suggested that up to 31±3% of the incorporated C was in substitutional sites.

Although the most stable configuration for C atoms in the Si lattice is the substitutional site,[9] Gall *et al.*[10] have demonstrated recently, using *ab initio* density-functional-theory-based calculations, that the situation is quite different for the case of C in Ge. They showed that the formation energy per C atom, $\tilde{U}=U/N_C$, continuously decreases with increasing number N_C of C atoms in a given configuration, from 2.42 eV for substitutional C, to 2.17 eV for a C pair on a single substitutional site, to 1.66 eV with $N_C=3$. This indicates that C has a strong tendency to form nanoclusters in Ge. Gall *et al.* also calculated the strain coefficient α for more than 50 C configurations in the Ge lattice and found that the absolute value of α is largest for single-C configurations $(N_C=1)$. For substitutional C, they obtained a strain coefficient $\alpha_{\rm sub}$ of -0.71 (slightly smaller than the Vegard's rule value), while α decreases to approximately zero for configurations with $N_C \geqslant 2$.

D'Arcy-Gall *et al.*[11] using a combination of calculated strain coefficients and layer strains measured by high-resolution x-ray diffraction (HR-XRD), provided evidence for C incorporation at nanocluster sites in $Ge_{1-y}C_y$/Ge(001) films grown from hyperthermal Ge and C atomic beams. Specifically, they showed that all C atoms are incorporated into both substitutional and Ge–C split interstitial sites at low y and T_s values with the relative concentrations controlled by the incident Ge-atom energy.[12] However, as y and/or T_s are increased, a growing fraction of C is incorporated in nanoclusters. Ge–C split interstitials are formed during growth from hyperthermal beams as a result of the trapping, by substitutional C, of Ge self-interstitials created by fast Ge irradiation.[12] For $Ge_{1-y}C_y$ growth from *thermal* beams, as in the present MBE experiments, self-interstitial, and hence Ge–C split interstitial, concentrations should be negligible. The formation energy of Ge–C split interstitials is 1.78 eV higher than that of substitutional C.[10]

In this article, we determine C lattice site distributions in Ge during MBE growth of epitaxial $Ge_{1-y}C_y$/Ge(001) alloys as a function of composition $(y \leqslant 0.045)$ and deposition temperature $(200 \leqslant T_s \leqslant 400\,^\circ C)$. To accomplish this, we employ a combination of high-resolution reciprocal lattice mapping (HR-RLM), cross sectional transmission electron microscopy (XTEM), and Raman spectroscopy. Based upon the results, together with previous *ab initio* density functional calculations,[10] C incorporation pathways during film growth are deduced.

We find that irrespective of y and T_s values, complete incorporation of C atoms in Ge substitutional sites is not possible; a fraction of the total C concentration is always incorporated in nanoclusters. The latter fraction increases with y and/or T_s due to correspondingly higher C–C encounter probabilities at the growth surface. Annealing as-deposited $Ge_{1-y}C_y$(001) layers results in a further loss in the substitutional concentration as C atoms migrate to nanocluster sites. This provides direct experimental evidence, confirming calculated results,[10] that the most energetically favorable configuration for C in the Ge lattice is in the form of nanoclusters.

II. EXPERIMENTAL PROCEDURE

All $Ge_{1-y}C_y$(001) alloy layers were grown in a multichamber solid-source MBE system, described in detail in Ref. 13, with a base pressure of 5×10^{-11} Torr. A pyrolytic BN effusion cell was used to evaporate 99.9999% pure Ge while pyrolytic graphite (purity=99.99%) was sublimed in a magnetically focused electron-beam evaporator. Surface structural and morphological changes were recorded *in situ* by reflection high-energy electron diffraction (RHEED) using a 20 keV primary electron beam which intercepts the sample at an angle of ≃2°.

The substrates are polished $1.5\times1.5\ cm^2$ Sb-doped Ge(001) wafers with room-temperature resistivities of $1-20\ \Omega$ cm $(n=1\times10^{15}-6\times10^{13}\ cm^{-3})$. Substrate cleaning consisted of ultrasonic degreasing, rinsing in deionized water to remove the native oxide, and oxidation by a UV-ozone process.[14] The wafers were then immediately inserted into the ultrahigh vacuum system. Final substrate preparation included degassing at 250 °C for 4 h and desorption of the oxide layer at 600 °C for 10 min. 500 Å-thick Ge(001) buffer layers were deposited at $T_s=400\,^\circ C$ followed by the growth of 1500 Å-thick $Ge_{1-y}C_y$(001) alloy layers at temperatures T_s between 200 and 400 °C. The Ge deposition rate was 0.4 Å s^{-1}, while the C deposition rate was set to obtain the desired alloy composition. Film growth temperatures were measured using a pyrometer calibrated by a thermocouple bonded to a dummy Ge substrate. The chamber pressure during deposition was $\leqslant 2\times10^{-9}$ Torr.

Deposited film thicknesses t were measured using microstylus profilometry while total C concentrations y in as-deposited layers were determined using a Cameca IMS-5F secondary-ion mass spectrometer (SIMS) operated with a 10 keV Cs^+ primary ion beam. Quantification, with an experimental uncertainty of ±10%, was carried out by comparison to C ion-implanted bulk Ge standards. All SIMS depth profiles were found to be flat showing that C concentrations remain constant as a function of depth in the $Ge_{1-y}C_y$(001) layers.

HR-XRD and HR-RLM measurements were performed using a Philips X-pert MRD diffractometer with Cu $K\alpha_1$ radiation (λ=1.540 597 Å) from a four-crystal Ge(220) monochromator which provided an angular divergence of <12 arc s with a wavelength spread $\Delta\lambda/\lambda \simeq 7\times10^{-5}$. ω–2θ scans (ω is the angle of incidence and θ is the Bragg diffraction angle) were obtained with a detector acceptance angle of ≃2°, while an additional two-crystal Ge(220) analyzer was placed between the sample and the detector for high-resolution scans (detector acceptance angle ≃12 arc s). HR-RLMs were generated by taking repetitive ω–2θ scans starting at different initial values for ω.

XTEM examinations were carried out using a Philips CM12 microscope operated at 120 keV. Specimens for XTEM examinations were prepared by gluing two samples

Downloaded 28 Feb 2002 to 130.126.102.15. Redistribution subject to AIP license or copyright, see http://ojps.aip.org/japo/japcr.jsp

film to film and then cutting a vertical section which was thinned by mechanical grinding to a thickness of $\simeq 25\ \mu m$. Final thinning to electron transparency was done by Ar^+ ion milling in which the incident beam angle and energy were progressively reduced from 15° to 9° and 5 to 3.5 keV in order to obtain samples with relatively uniform thickness distributions.

Raman measurements were performed using the 5145 Å line from an Ar^+ ion laser. The 40 mW laser beam was incident at 60° to the sample normal and focused to a spot size of $\simeq 300\ \mu m$. The optical penetration depth at this wavelength is $\simeq 160$ Å,[15] much smaller than the alloy layer thickness. A three-stage 0.8 m SPEX spectrometer equipped with a two-dimensional (2D) charged-coupled device array was used to collect the signal perpendicular to the sample surface. Wavelength calibration was accomplished using a Ne lamp.

Annealing experiments were carried out at atmospheric pressure in ultrahigh purity Ar (99.999%). Following sample introduction, the annealing chamber was purged with Ar for 3 h. The samples were then rapidly heated at $\simeq 8\ °C\ s^{-1}$ to the annealing temperature T_a, held for 30 min, and cooled in Ar to room temperature. All samples were successively annealed at temperatures of 450 °C, 550 °C, and 650 °C.

III. EXPERIMENTAL RESULTS

A. Film growth

Epitaxial $Ge_{1-y}C_y$ layers with nominal thicknesses $t = 1500$ Å and concentrations $y \leqslant 0.045$ were grown on Ge(001) at $T_s = 200–400$ °C in order to probe C incorporation pathways. We used HR-RLM to show that all $Ge_{1-y}C_y(001)$ layers are fully coherent with their substrate. SIMS analyses were performed on all films.

Typical zero-order Laue-zone RHEED patterns are presented in Fig. 1. Patterns from Ge(001) buffer layers [Fig. 1(a)] consist of sharp 2×1 spots, with nearly equi-intense fundamental and half-order features and sharp Kikuchi lines characteristic of a flat surface. Upon initiating growth of $Ge_{1-y}C_y(001)$ alloys with $y \leqslant 0.023$ at $T_s \leqslant 300$ °C, RHEED features become streaky, half-order intensities decrease, diffuse scattering increases, and the fundamental diffraction rods broaden. These effects are indicative of decreasing average terrace sizes, increasing step densities, and atomic-scale surface roughening. Typical patterns from 1500 Å-thick $Ge_{0.977}C_{0.023}(001)$ layers grown at $T_s = 200$ and 300 °C are shown in Figs. 1(b) and 1(c), respectively. The layers remain 2D and show no evidence of faceting, in agreement with XTEM analyses described in the following section. However, RHEED patterns from $Ge_{1-y}C_y(001)$ layers with C concentrations $y \geqslant 0.035$ gradually transform from 2D to three-dimensional (3D) with increasing thickness. For example, 3D patterns are obtained from $y = 0.035$ alloys grown at $T_s = 200$ °C when the film thickness exceeds 515 Å.

RHEED patterns acquired during $Ge_{1-y}C_y(001)$ growth at $T_s \geqslant 350$ °C reveal increased surface roughening together with evidence for faceting. The half-order streaks rapidly disappear, resulting in 1×1 patterns, at thicknesses ranging

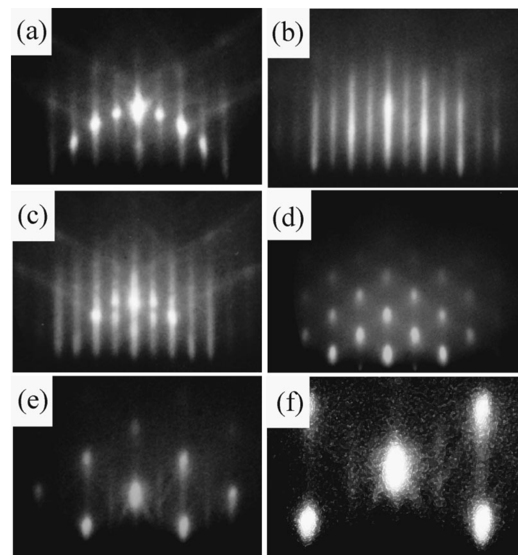

FIG. 1. RHEED patterns from (a) a 500 Å-thick Ge buffer layer grown at $T_s = 400$ °C and 1500 Å-thick $Ge_{0.977}C_{0.023}$ alloy layers grown by MBE on Ge(001) at temperatures T_s: (b) 200 °C, (c) 300 °C, (d) 350 °C, and (e) 400 °C. (f) Enlarged section of the RHEED pattern in (e) showing chevron-shaped streaks emanating from the diffraction spots.

from $t \simeq 1500$ Å with $y = 0.012$ to $t \simeq 680$ Å with $y = 0.023$ at $T_s = 350$ °C. In parallel, vertical intensity modulations become visible along the length of the fundamental diffraction rods. With further increases in film thickness, the modulated 1×1 pattern gradually transforms into a bulk 3D pattern such as the one shown in Fig. 1(d), obtained from a 1500 Å-thick $Ge_{0.977}C_{0.023}(001)$ layer grown at $T_s = 350$ °C. Increasing T_s to 400 °C yields extremely rough surfaces with RHEED patterns exhibiting streaks corresponding to the presence of {113} facets with $t > 440$ Å. The chevron-shaped streaks emanate from both the tops and bottoms of diffraction features [see Figs. 1(e) and 1(f), obtained from a $Ge_{0.977}C_{0.023}(001)$ alloy grown at $T_s = 400$ °C with $t = 1500$ Å), and are inclined 25° with respect to the surface normal.

B. Microstructure and strain state

In this section, we describe the effect of T_s on film microstructure and strain state and then consider the influence of alloy composition for films grown at $T_s = 200$ °C, the minimum growth temperature used. We choose $Ge_{0.977}C_{0.023}(001)$ alloys to illustrate the effect of T_s on microstructure and C lattice site distributions since, while $y = 0.023$ represents a relatively high C concentration, the alloys remain of excellent crystalline quality over a wide range in growth temperature.

Figures 2(a) and 2(b) are typical bright-field XTEM images, obtained using the $\bar{g} = 220$ diffraction vector near the 110 zone axis, from fully strained 1500 Å-thick $Ge_{0.977}C_{0.023}(001)$ layers grown at $T_s = 200$ and 400 °C, respectively. The film/buffer-layer interfaces are abrupt (as determined using $\bar{g} = 200$ imaging conditions) and there is no evidence for stacking faults, misfit dislocations, or C precipitates (detection limit $\simeq 50$ Å), in agreement with the HR-RLM results presented next. 110 zone axis selected-area

Downloaded 28 Feb 2002 to 130.126.102.15. Redistribution subject to AIP license or copyright, see http://ojps.aip.org/japo/japcr.jsp

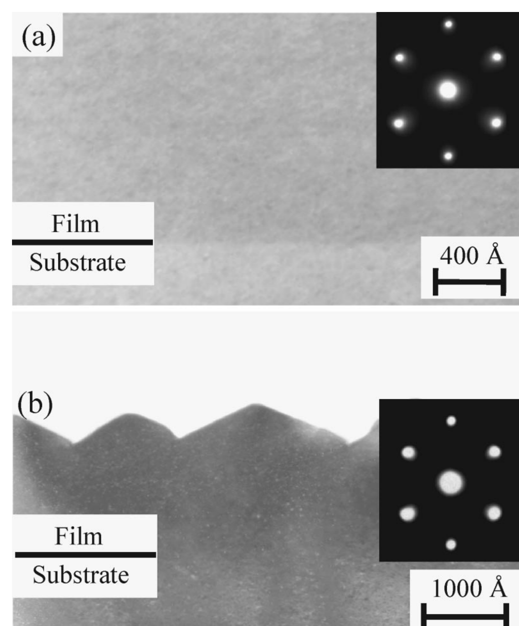

FIG. 2. Bright-field XTEM images, obtained with diffraction vector $\bar{g} = 220$ near [110], from fully coherent 1500 Å-thick $Ge_{0.977}C_{0.023}$ alloy layers grown on Ge(001) at temperatures T_s of (a) 200 °C and (b) 400 °C. 110 SAED patterns are shown in the insets of (a) and (b).

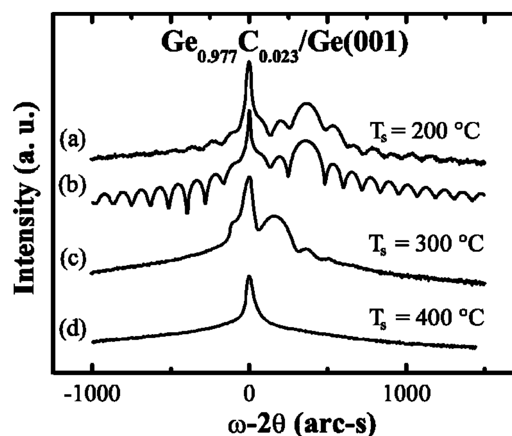

FIG. 3. HR-XRD ω–2θ scans through the 004 Bragg peaks from $Ge_{0.977}C_{0.023}$ alloy layers grown on Ge(001) at (a) $T_s = 200$ °C, (c) 300 °C, and (d) 400 °C. (b) A fully dynamical simulation of the HR-XRD scan in (a). The curves are shifted vertically for clarity.

electron-diffraction (SAED) patterns [see for example, the insets in Figs. 2(a) and 2(b)] are composed of single-crystal reflections with symmetric intensities.

Consistent with the RHEED results, XTEM analyses reveal that surfaces of $Ge_{0.977}C_{0.023}(001)$ layers grown at $T_s = 200$ °C [Fig. 2(a)] remain flat to within the resolution of the transmission electron microscopy. However, alloys with $y \geqslant 0.023$ grown at $T_s \geqslant 350$ °C exhibit extensive surface roughening and facet formation as shown in Fig. 2(b). The roughening is C induced since we find that the surfaces of pure Ge(001) layers grown to the same thicknesses at $T_s = 350$–400 °C are flat. The peak to valley roughness for the Fig. 2(b) layer is 500 Å. The angle between [001] and a vector orthogonal to facet surfaces is 25.2°, indicating, as observed in RHEED patterns, that the facets are terminated by {113} planes.

Typical HR-XRD ω–2θ scans through substrate and film 004 Bragg peaks are presented in Fig. 3 for $Ge_{0.977}C_{0.023}$ layers grown at $T_s = 200$, 300, and 400 °C. Figure 3(a) is from a 1500 Å-thick, $y = 0.023$ alloy grown at $T_s = 200$ °C. The diffraction pattern exhibits a sharp layer peak, with a full width at half maximum intensity $\Gamma_{\omega-2\theta}$ in the ω–2θ direction of 111 arc s, in good agreement with the theoretical minimum value, accounting for strain broadening and finite thickness effects,[16,17] of 107 arc s. This indicates that the film is of very high crystalline quality. The positive angular separation between substrate and layer peaks, $\Delta\omega = 360$ arc s, demonstrates that the film is in a state of in-plane tension with an out-of-plane lattice constant $a_\perp = 5.6408$ Å. Our measured $a_\perp$ value is considerably larger than the lattice constant, $a_\perp = 5.5652$ Å, obtained by assuming all C atoms reside in substitutional sites and applying the corresponding strain coefficient $\alpha_{sub} = -0.71$.[10] This result, combined with the fact that the layer is fully coherent, suggests that only a small fraction of incorporated C resides on substitutional sites.

Finite-thickness interference fringes are clearly visible in Fig. 3(a), indicating that the layer is of high structural quality with a laterally uniform substrate/film interface. This is consistent with the XTEM results in Fig. 2(a). From the fringe spacing, we obtain a layer thickness of 1485 Å, in good agreement with growth rate calibrations. A simulated HR-XRD scan, calculated based upon the fully dynamical formalism of Tagaki[16] and Taupin,[17] is shown in Fig. 3(b) for comparison. The simulation was carried out assuming a perfectly abrupt and coherent film/buffer-layer interface with all C atoms residing in substitutional sites. Reproducing the measured Bragg and fringe peak positions in the simulation, using the assumption (verified below) that nonsubstitutional C atoms exert negligible in-plane strain in the Ge lattice,[10] yields a substitutional C concentration of only 0.42 at. % while the total measured C concentration is 2.3 at. %. The intensities of the calculated Bragg peaks and interference fringes [Fig. 3(b)] are in good agreement with measured results [Fig. 3(a)].

Increasing T_s to 300 °C while maintaining the total C concentration at 2.3 at. % decreases the degree of in-plane tension as shown in Fig. 3(c), from which we obtain $a_\perp = 5.6508$ Å. $\Gamma_{\omega-2\theta}$ for this 1300 Å-thick layer is 131 arc s, somewhat larger than the calculated value of 111 arc s and indicative of a slight decrease in crystalline quality. However, finite-thickness interference fringes are still visible near the substrate and layer peaks. In contrast, HR-XRD scans from $Ge_{0.977}C_{0.023}(001)$ alloys grown at $T_s = 400$ °C [see, for example, Fig. 3(d)] exhibit no distinct layer peak demonstrating that these layers contain negligible substitutional C.

All $Ge_{1-y}C_y(001)$ alloy layers are completely coherent with their substrates as determined from XTEM and HR-RLM analyses. Representative reciprocal lattice maps around asymmetric 224 reflections are presented in Fig. 4. Diffracted intensity distributions are plotted as isointensity contours as a function of the reciprocal lattice vectors $k_\parallel$ parallel and $k_\perp$ perpendicular to the surface. The substrate and film peaks from all samples in this study, irrespective of y and T_s, are

Downloaded 28 Feb 2002 to 130.126.102.15. Redistribution subject to AIP license or copyright, see http://ojps.aip.org/japo/japcr.jsp

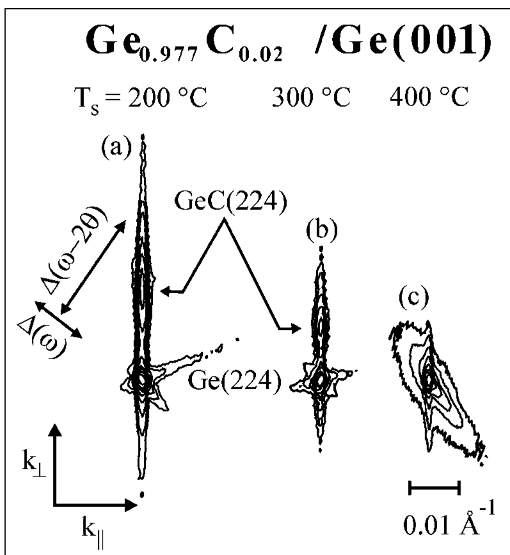

FIG. 4. HR-RLMs around asymmetric 224 Bragg peaks from $Ge_{0.977}C_{0.023}$ alloys grown on Ge(001) at (a) $T_s = 200\,°C$, (b) 300 °C, and (c) 400 °C.

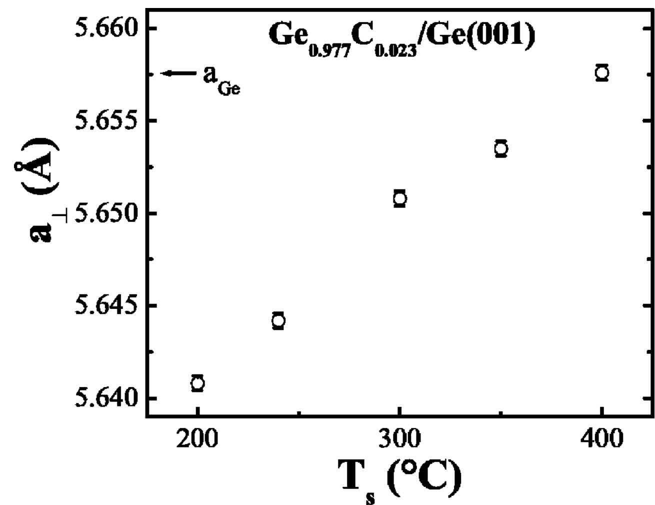

FIG. 5. Lattice parameter $a_\perp$ along the film growth direction vs the deposition temperature T_s for $Ge_{0.977}C_{0.023}$ alloy layers grown on Ge(001).

aligned along the $k_\parallel$ direction signifying negligible in-plane strain relaxation. The diffraction contours in Fig. 4 are nearly symmetric with the exception of the elongation, due to finite-thickness effects, along the growth direction.

The HR-RLM in Fig. 4(a) was obtained from a 1500 Å-thick $Ge_{0.977}C_{0.023}(001)$ alloy grown at $T_s = 200\,°C$. The layer is under tensile strain with an out-of-plane lattice constant $a_\perp = 5.6411$ Å, in good agreement with the HR-XRD results ($a_\perp = 5.6408$ Å). The full width at half maximum intensity in the ω and ω–2θ directions for the layer peak are $\Gamma_\omega = 54$ and $\Gamma_{\omega-2\theta} = 43$ arc s, close to the substrate values of 35 and 37 arc s indicating negligible film mosaicity and microstrain. Finite-thickness interference fringes are clearly visible as periodic intensity contours along $k_\perp$. The diffraction intensity distribution passing transversely through the substrate peak is due to residual scattering from the monochromator crystal.

Figure 4(b) is an HR-RLM from a $Ge_{0.977}C_{0.023}(001)$ alloy grown at $T_s = 300\,°C$. The substrate and layer peaks are again nearly perfectly aligned along $k_\parallel$ with an in-plane strain relaxation of only 2.5×10^{-5}, near the instrument detection limit of $\simeq 1 \times 10^{-5}$. The layer is under tensile strain with a lattice constant along the growth direction of $a_\perp = 5.6514$ Å. Γ_ω and $\Gamma_{\omega-2\theta}$ for the layer peak are 61 arc s and 63 arc s, respectively, corresponding to a slight decrease in crystalline quality compared to the $T_s = 200\,°C$ results. Increasing T_s to 400 °C causes the layer peak to merge with that of the substrate suggesting the absence of C in substitutional lattice sites. The diffuse scattering intensity at angles away from the Bragg peak is high signifying large variations in the local microstrain induced by C incorporated in nanocluster sites (see below) which cause severe lattice-plane buckling distortions.

Since all $Ge_{1-y}C_y$/Ge(001) alloys in this investigation are fully coherent with their Ge substrates, their out-of-plane lattice constant depends only on C lattice site distributions. Figure 5 is a plot of $a_\perp$ for $Ge_{0.977}C_{0.023}(001)$ layers deposited as a function of growth temperature T_s. $a_\perp(T_s)$ increases nearly linearly from 5.6408 Å at $T_s = 200\,°C$ to 5.6576 Å, equal to the bulk substrate value a_{Ge}, at 400 °C. All data points in Fig. 5, irrespective of T_s, are well above the value, $a_\perp = 5.5652$ Å, calculated using the strain coefficient $\alpha_{sub} = -0.71$[10] corresponding to fully substitutional C incorporation.

Figure 6 shows out-of-plane lattice constants $a_\perp$ for $Ge_{1-y}C_y(001)$ layers grown at $T_s = 200$ and 300 °C as a function of the total C concentration y. The data clearly exhibit two distinct regimes. At low C concentrations ($y \leq 0.023$ at 200 °C and $y \leq 0.013$ at 300 °C), $a_\perp$ decreases with increasing y to reach a minimum value of 5.6408 Å at 200 °C and 5.6466 Å at 300 °C. $a_\perp$ then increases again at higher C concentrations to saturate at the lattice constant of bulk Ge, a_{Ge}. The dashed line in Fig. 6 corresponds to the calculated alloy lattice constant for fully substitutional C in-

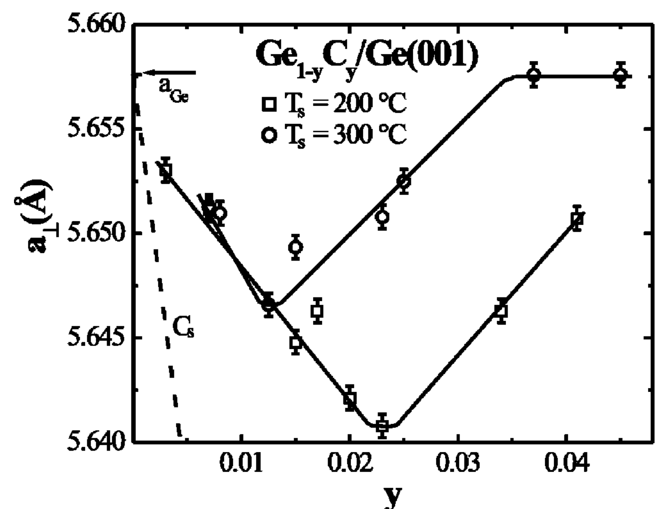

FIG. 6. Lattice parameters $a_\perp$ along the film growth direction vs the total C concentration y in $Ge_{1-y}C_y$/Ge(001) alloy layers grown at $T_s = 200$ and 300 °C. The dashed line represents calculated $a_\perp(y)$ values assuming C incorporates solely in substitutional lattice sites.

Downloaded 28 Feb 2002 to 130.126.102.15. Redistribution subject to AIP license or copyright, see http://ojps.aip.org/japo/japcr.jsp

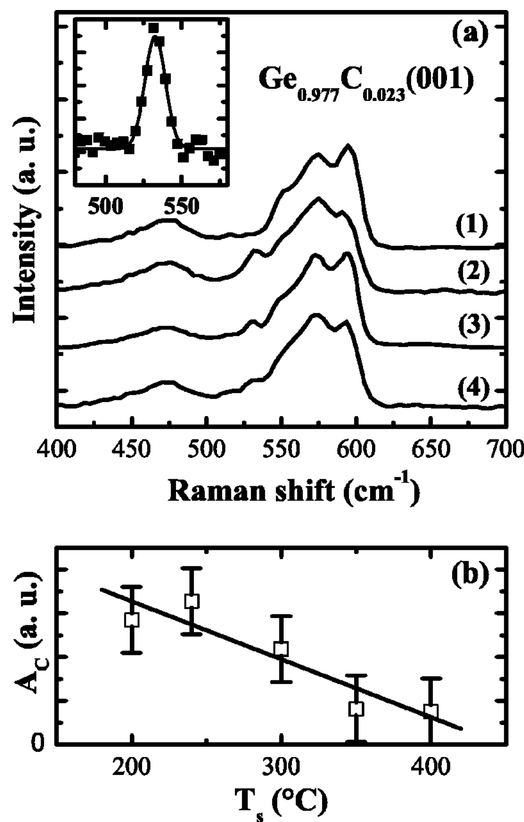

FIG. 7. (a) Raman spectra obtained from (1) a bulk Ge(001) wafer and $Ge_{0.977}C_{0.023}(001)$ alloys grown on Ge(001) at (2) $T_s = 200\,°C$, (3) $T_s = 350\,°C$, and (4) $T_s = 200\,°C$ and annealed for 30 min at $T_a = 550\,°C$. The inset is a plot of the normalized C 531 cm^{-1} LVM peak from curve 2 fitted with a Gaussian (solid line). (b) The integrated areas A_C under the substitutional C LVM Raman peaks from $Ge_{0.977}C_{0.023}(001)$ alloys grown on Ge(001) as a function of T_s.

corporation. All data points are well above this line indicating that significant fractions of incorporated C atoms occupy non-substitutional sites.

C. Raman spectroscopy measurements

$Ge_{1-y}C_y/Ge(001)$ layers were also probed by Raman spectroscopy. Substitutional C atoms in the Ge lattice are known to give rise to a local vibrational mode (LVM) which has previously been reported to occur at approximately 531 cm^{-1}.[7,8] Curve 1 in Fig. 7(a) is a reference Raman spectrum, over the Stokes shift range between 400 and 700 cm^{-1}, from a Ge(001) substrate. We attribute the 595 cm^{-1} peak to two-phonon intensity close to the Brillouin zone center.[18] The peak at 575 cm^{-1} is due to a high transverse optical (TO) phonon density of states near the X point in the Ge phonon dispersion curve,[18] while the shoulder at 550 cm^{-1} is related to a two-phonon process involving one longitudinal (LO) and one transverse optical (TO) mode. The feature near 467 cm^{-1} corresponds to a convolution of the Ge two-phonon longitudinal optical and acoustic (LA) modes.[18]

Curves 2 and 3 in Fig. 7(a) are typical Raman spectra, in this case from $Ge_{0.977}C_{0.023}(001)$ alloy layers grown at $T_s = 200\,°C$ and $350\,°C$, respectively. The spectra contain an additional peak corresponding to the 531 cm^{-1} LVM from

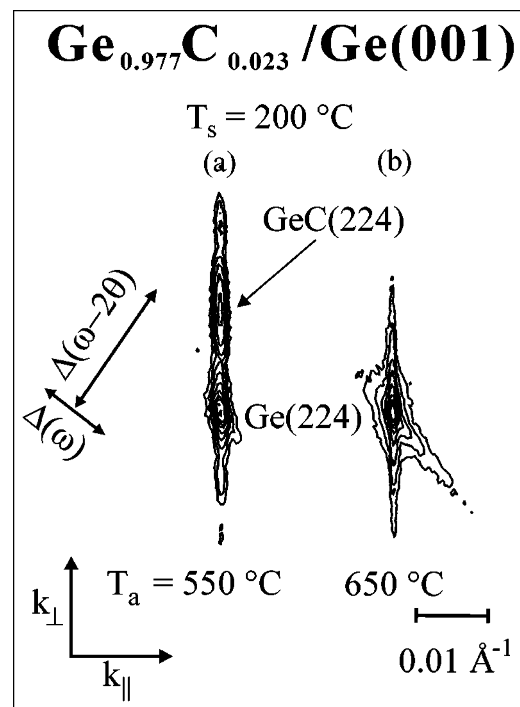

FIG. 8. HR-RLMs around asymmetric 224 Bragg peaks from a 1500 Å-thick $Ge_{0.977}C_{0.023}$ alloy grown on Ge(001) at $T_s = 200\,°C$ and successively annealed for 30 min at $T_a = 450\,°C$, (a) 550 °C, and (b) 650 °C.

substitutional C in Ge.[7,8,11] We note that the area under the C peak from the $T_s = 350\,°C$ sample is smaller than that of the 200 °C alloy. In order to compare results as a function of y and T_s, all Raman spectra were normalized to the Ge 2TO peak intensity at 595 cm^{-1} and the pure Ge spectra subtracted. The C-related peaks were then well fit using a Gaussian function centered at 531 cm^{-1}. An example fit, in this case for the sample shown in curve 2, is given in the inset of Fig. 7(a). The integrated area A_C under the C peak from $Ge_{0.977}C_{0.023}(001)$ alloys is plotted as a function of T_s in Fig. 7(b). We find that A_C decreases with increasing film growth temperature. Since the C peak area is directly proportional to the substitutional C concentration incorporated in the $Ge_{1-y}C_y(001)$ layers, the results show that y_{sub} decreases approximately linearly with increasing T_s, consistent with our HR-RLM measurements (Fig. 4).

D. Annealing effects on C lattice site distributions

Annealing experiments were carried out in order to investigate the thermal stability of $Ge_{1-y}C_y(001)$ alloys. All samples were successively annealed in Ar at temperatures T_a of 450, 550, and 650 °C for 30 min. Changes in alloy lattice constants were determined by HR-XRD and HR-RLM after each step. All layers remained fully coherent and SIMS C depth profiles were found to be identical to those obtained from as-deposited samples.

A typical set of HR-RLMs from an annealed 1500 Å-thick $Ge_{0.977}C_{0.023}(001)$ alloy grown at $T_s = 200\,°C$ is shown in Fig. 8. The substrate and the film peaks remain perfectly aligned along the $k_\parallel$ direction signifying negligible in-plane strain relaxation. In fact, the 450 °C anneal had no

Downloaded 28 Feb 2002 to 130.126.102.15. Redistribution subject to AIP license or copyright, see http://ojps.aip.org/japo/japcr.jsp

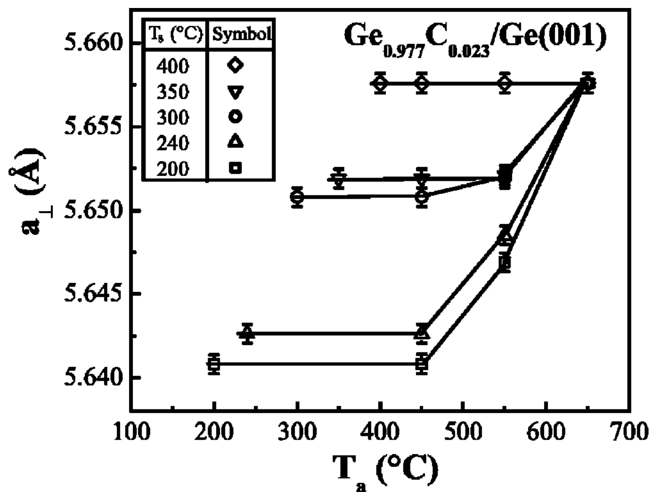

FIG. 9. Lattice parameters $a_\perp$ along the film growth direction as a function of the annealing temperature T_a for 1500 Å-thick $Ge_{0.977}C_{0.023}$ alloys grown on Ge(001) at $T_s = 200\,°C - 400\,°C$.

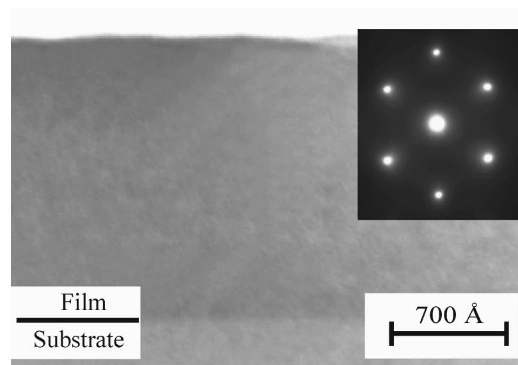

FIG. 10. A bright-field XTEM image, obtained with $\bar{g} = 220$ near [110], from the $Ge_{0.977}C_{0.023}(001)$ alloy corresponding to Fig. 2(a) after annealing for 30 min at $T_a = 650\,°C$.

measurable effect whatsoever, with the HR-RLM remaining identical to that shown in Fig. 4(a). However, at $T_a = 550\,°C$, the layer peak in the HR-RLM moves closer to the Ge substrate peak, as $a_\perp$ increases from 5.6408 to 5.6472 Å, corresponding to a lower tensile strain. We obtain Γ_ω and $\Gamma_{\omega-2\theta}$ values of 41 arc s and 39 arc s, respectively, slightly lower than in the as-deposited sample (54 and 43 arc s). This is indicative of a slight increase in crystalline quality, associated with a decrease in the overall tensile strain, and changes in C lattice site distributions. Annealing at $T_a = 650\,°C$ relieves the remaining tensile strain such that $a_\perp = a_\parallel = a_{Ge}$, as shown in Fig. 8(b).

$a_\perp$ values are plotted as a function of T_a in Fig. 9 for $Ge_{0.977}C_{0.023}(001)$ layers grown at $T_s = 200-400\,°C$. For each curve, the data point at the lowest temperature corresponds to $a_\perp$ for the as-deposited layer. The results clearly show that 450 °C anneals have no effect on $a_\perp$, irrespective of T_s. Increasing T_a to 550 °C, however, leads to an increase in $a_\perp$ for alloys grown at $T_s = 200-300\,°C$, while $a_\perp$ remains constant for $Ge_{0.977}C_{0.023}(001)$ films grown at $T_s \geqslant 350\,°C$. Annealing at $T_a = 650\,°C$ reduces the residual strain to zero ($a_\perp = a_{Ge}$) for all layers, suggesting that the substitutional C concentrations in these layers become negligible.

We provide further evidence from Raman spectroscopy for a decrease in substitutional C concentration upon annealing. Curve 4 in Fig. 7(a) is a Raman spectrum obtained from a $Ge_{0.977}C_{0.023}(001)$ layer grown at $T_s = 200\,°C$ [curve 2 in Fig. 7(a)] and annealed at $T_a = 550\,°C$. The integrated area A_C under the C peak has decreased by approximately a factor of 2 during annealing, indicating a corresponding decrease in the substitutional C concentration. This is consistent with the HR-RLM results showing that annealing leads to a decrease in tensile strain and indicates that substitutional C atoms migrate during annealing to sites which exert negligible lattice strain.

An XTEM bright-field image, obtained using a $\bar{g} = 220$ diffraction vector near the 110 zone axis, from a $Ge_{0.977}C_{0.023}(001)$ alloy grown at $T_s = 200\,°C$ and annealed at $T_a = 650\,°C$ is presented in Fig. 10. The annealed film still contains no observable stacking faults, dislocations, or evidence for C precipitates, and the substrate/film interface remains abrupt. This suggests that changes in layer strain are related solely to changes in C lattice site distributions, rather than, for example, C decoration of extended defects. From our strain results (Fig. 5), this as-deposited $Ge_{0.977}C_{0.023}(001)$ sample had the highest substitutional C concentration, $y_{sub} = 0.0042$. However, the corresponding tensile strain was completely relaxed during the 650 °C annealing.

IV. DISCUSSION

$Ge_{1-y}C_y(001)$ alloys grown by MBE at $T_s = 200-400\,°C$ with C concentrations up to 4.5 at. % are of high crystalline quality and fully coherent with their Ge(001) substrates as judged by RHEED, HR-XRD, HR-RLM, and XTEM. Total incorporated C concentrations y obtained from quantitative SIMS measurements agree well with values expected from growth rate calibrations and were found to be independent of T_s.

In situ RHEED and XTEM analyses showed that all $Ge_{1-y}C_y(001)$ layers grown at $200 \leqslant T_s \leqslant 300\,°C$ with $y < 0.035$ have smooth 2×1 surfaces and contain no extended defects. However, layers grown at $T_s \geqslant 350\,°C$ exhibit significant surface roughness with, at $T_s = 400\,°C$, the development of {113} facets as observed by both RHEED and XTEM. {113}-faceted epitaxial and amorphous $Ge_{1-y}C_y$ layers grown on Ge(001) were previously reported by D'Arcy-Gall *et al.*[19] and Yang *et al.*,[3] respectively. C-induced {113} facets have also been observed during the homoepitaxial growth of Si(001),[20] and attributed, based on *ab initio* density functional calculations, to the stabilization of {113} facets by C atoms which tend to favor sp^2 rather than sp^3 hybridization.[21]

$Ge_{1-y}C_y(001)$ alloys grown on Ge(001) at $T_s = 200\,°C$ are in a state of in-plane tensile strain whose magnitude, as determined by HR-XRD and HR-RLM, decreases linearly with increasing T_s until it becomes negligible for all alloy compositions at $T_s = 400\,°C$. Consistent with these results, Raman spectroscopy analyses provide direct experimental evidence showing that the fraction of the total C concentra-

Downloaded 28 Feb 2002 to 130.126.102.15. Redistribution subject to AIP license or copyright, see http://ojps.aip.org/japo/japcr.jsp

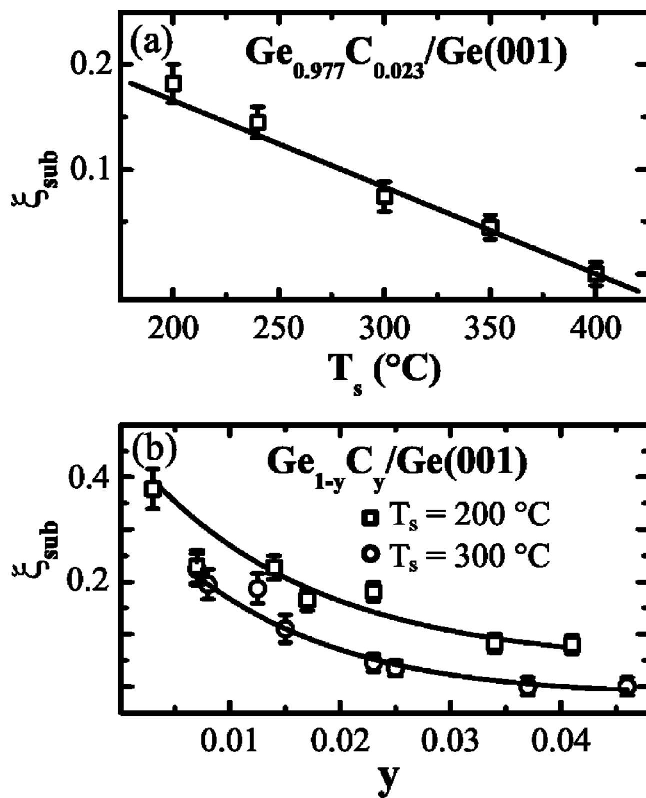

FIG. 11. (a) The fraction ξ_{sub} of C incorporated in substitutional sites in $Ge_{0.977}C_{0.023}$/Ge(001) alloys as a function of the growth temperature T_s. (b) ξ_{sub} as a function of the total C concentration y in $Ge_{1-y}C_y$(001) alloys grown on Ge(001) at $T_s = 200\,^\circ$C and 300 °C.

tion which is incorporated in substitutional lattice sites also decreases linearly with increasing T_s. Based upon previous results using hyperthermal atom beams,[11,12] the only significant nonsubstitutional C sites in $Ge_{1-y}C_y$/Ge(001) are Ge–C split interstitials, whose concentration is expected to be insignificant in the present MBE experiments, and C nanoclusters which induce negligible strain in the Ge lattice ($\alpha_{cluster} = 0$). Thus, the out-of-plane lattice constant $a_\perp$ of fully coherent $Ge_{1-y}C_y$ films on Ge(001) depends solely on the substitutional C concentration y_{sub} in the alloys, weighted by the strain coefficient $\alpha_{sub} = -0.71$. Thus, $a_\perp$ is related to y_{sub} through the simple relationship,

$$a_\perp = a_{Ge}(1 + \alpha_{sub} y_{sub}). \quad (1)$$

Using Eq. (1) together with our measured $a_\perp$ values, the total C concentration y obtained by SIMS, and the calculated strain coefficients, we extract the substitutional C fraction $\xi_{sub} = y_{sub}/y$ in our $Ge_{1-y}C_y$ (001) layers. Figure 11(a) is a plot of ξ_{sub} as a function of T_s for $Ge_{0.977}C_{0.023}$(001) films. ξ_{sub} decreases approximately linearly from a maximum value of 0.18 at $T_s = 200\,^\circ$C to become essentially zero at $T_s = 400\,^\circ$C. Figure 11(b) shows the substitutional C fraction as a function of the total C concentration y in $Ge_{1-y}C_y$(001) alloys grown at $T_s = 200\,^\circ$C and 300 °C. We obtain the highest substitutional C fraction, $\xi_{sub} = 0.38$, for $Ge_{0.997}C_{0.003}$/Ge(001) layers grown at 200 °C. Increasing y leads to a continuous decrease in ξ_{sub} to 0.08 with $y = 0.041$. We observe the same trend in the 300 °C layers, but with lower absolute values for ξ_{sub}. Overall, the substitutional C fraction is small in all $Ge_{1-y}C_y$(001) alloys, irrespective of y *and* T_s. This is consistent with *ab initio* density functional calculations showing that C incorporation in nanocluster sites is energetically favored over incorporation in substitutional Ge lattice sites.[10] The fact that we observe $\xi_{cluster} = (1 - \xi_{sub})$ increasing with y as well as T_s suggests that nanocluster formation is kinetically limited during film deposition by the C–C adatom encounter probability at the growth surface.

No changes were observed in either the in-plane strain or the area A_C under the C LVM Raman peak during 30 min anneals of $Ge_{0.977}C_{0.023}$(001) layers at $T_a = 450\,^\circ$C. At higher annealing temperatures, however, $a_\perp$ increases while A_C, and hence the substitutional C concentration, decreases. The alloy layers remain fully coherent with their Ge(001) substrates and free of extended defects. Thus, 30 min at $T_a \geqslant 550\,^\circ$C is sufficient to induce C diffusion from substitutional lattice sites to lower-energy nanocluster sites. At $T_a = 650\,^\circ$C, all residual substitutional C is lost. Using the reported activation energy for substitutional C diffusion in Ge, 2.6 eV,[5] we estimate C mean diffusion distances in our $Ge_{1-y}C_y$(001) layers during 30 min anneals at 450, 550, and 650 °C, to be <1 Å, 11 Å, and 85 Å, respectively, which are consistent with our experimental results. For $Ge_{1-y}C_y$(001) alloys with $y = 0.023$, substitutional C atoms are separated by $\simeq 10$ Å. Thus, we observe negligible change in $a_\perp$ or ξ_{sub} values at $T_a = 450\,^\circ$C while a fraction of the substitutional C migrates to nanocluster sites at 550 °C (see Fig. 9), and all substitutional C is converted at $T_a = 650\,^\circ$C.

V. CONCLUSIONS

MBE $Ge_{1-y}C_y$ alloys grown at temperatures $T_s = 200$–$400\,^\circ$C with total C concentrations up to 4.5 at. % are fully commensurate with their Ge(001) substrates. HR-RLM and XTEM analyses show that the layers contain no detectable extended defects or C precipitates. We find that C atoms incorporate into *both* substitutional and nanoclusters sites. The combination of SIMS, HR-XRD, HR-RLM, and Raman spectroscopy, together with the results of previous *ab initio* density functional calculations,[10] were used to quantitatively determine, as a function of film growth conditions, the concentrations of C incorporated in each site.

We find that, in contrast to $Si_{1-y}C_y$ alloys grown on Si(001), it is not possible by MBE to obtain fully substitutional C incorporation in $Ge_{1-y}C_y$(001) alloys, irrespective of y and T_s. We attribute this to the fact that while substitutional C is the most energetically stable configuration in Si, C nanoclusters are the lowest energy sites in the Ge lattice. ξ_{sub} in $Ge_{1-y}C_y$(001) decreases with increasing T_s and/or y suggesting that the formation of nanoclusters is kinetically limited by the C–C adatom encounter probability at the growth surface.

All $Ge_{1-y}C_y$(001) layers are stable to 30 min anneals at $T_s = 450\,^\circ$C. However, annealing the alloys at $T_a = 550\,^\circ$C leads to a significant decrease in tensile strain while 650 °C annealed layers are strain and defect free as all substitutional C migrates to lower-energy nanocluster sites.

Downloaded 28 Feb 2002 to 130.126.102.15. Redistribution subject to AIP license or copyright, see http://ojps.aip.org/japo/japcr.jsp

ACKNOWLEDGMENTS

The authors gratefully acknowledge the financial support the Materials Science Division of the Department of Energy under Contract No. DEFG02-91ER45439. They also appreciate the use of the facilities of the Center for Microanalysis of Materials, which is partially supported by DOE, at the University of Illinois. One of the authors (P.D.) acknowledges support from the Canada Research Chair program, the Natural Sciences and Engineering Research Council of Canada, and the Fonds pour la Formation de chercheurs et à l'aide à la recherche (Québec, Canada).

[1] R. I. Scace and G. A. Slack, J. Chem. Phys. **30**, 1551 (1959).
[2] J. Tersoff, Phys. Rev. Lett. **74**, 5080 (1995).
[3] B. K. Yang, M. Krishnamurthy, and W. H. Weber, J. Appl. Phys. **82**, 3287 (1997).
[4] See for example J. Kolodzey, P. A. O'Neil, S. Zhang, B. A. Orner, K. Roe, K. M. Unruh, C. P. Swann, M. M. Waite, and S. Ismat Shah, Appl. Phys. Lett. **67**, 1865 (1995); M. Todd, J. Kouvetakis, and D. J. Smith, *ibid.* **68**, 2407 (1996)
[5] R. Duschl, O. G. Schmidt, W. Winter, K. Eberl, M. W. Dashiell, J. Kolodzey, N. Y. Jin-Phillipp, and F. Phillipp, Appl. Phys. Lett. **74**, 1150 (1999).
[6] M. W. Dashiell, J. Kolodzey, P. Boucaud, Vy Yam, and J.-M. Lourtioz, J. Vac. Sci. Technol. B **18**, 1728 (2000).
[7] W. H. Weber, B.-K. Yang, and M. Krishnamurthy, Appl. Phys. Lett. **73**, 626 (1998).
[8] L. Hoffman, J. C. Bach, B. Bech Nielsen, P. Leary, R. Jones, and S. Öberg, Phys. Rev. B **55**, 11167 (1997).
[9] J. Tersoff, Phys. Rev. Lett. **64**, 1757 (1990).
[10] D. Gall, J. D'Arcy-Gall, and J. E. Greene, Phys. Rev. B **62**, R7723 (2000).
[11] J. D'Arcy-Gall, D. Gall, P. Desjardins, I. Petrov, and J. E. Greene, J. Appl. Phys. **90**, 3910 (2001).
[12] J. D'Arcy-Gall, D. Gall, P. Desjardins, I. Petrov, and J. E. Greene, Phys. Rev. B **62**, 11203 (2000).
[13] O. Gurdal, P. Desjardins, J. R. A. Carlsson, N. Taylor, H. H. Radamson, J.-E. Sundgren, and J. E. Greene, J. Appl. Phys. **83**, 162 (1998).
[14] X.-J. Zhang, G. Xue, A. Agarwal, R. Tsu, M.-A. Hasan, J. E. Greene, and A. Rockett, J. Vac. Sci. Technol. A **11**, 2553 (1993).
[15] D. E. Aspnes and A. A. Studna, Phys. Rev. B **27**, 985 (1983).
[16] S. Tagaki, Acta Crystallogr. **15**, 1311 (1962).
[17] D. Taupin, Bull. Soc. Fr. Mineral. Cristallogr. **87**, 469 (1964).
[18] P. Brüesch, *Phonons: Theory and Experiments I* (Springer, 1982), p. 129.
[19] J. D'Arcy-Gall, P. Desjardins, I. Petrov, J. E. Greene, J.-E. Paultre, R. A. Masut, S. C. Gujrathi, and S. Roorda, J. Appl. Phys. **88**, 96 (2000).
[20] A. Oshiyama, Phys. Rev. Lett. **74**, 130 (1995).
[21] D. M. Bird, L. J. Clarke, R. D. King-Smith, M. C. Payne, I. Stich, and A. P. Sutton, Phys. Rev. Lett. **69**, 3785 (1992).

Downloaded 28 Feb 2002 to 130.126.102.15. Redistribution subject to AIP license or copyright, see http://ojps.aip.org/japo/japcr.jsp